

**CHEMOSTRATIGRAPHY AND MINERALOGY OF THE JEZERO WESTERN FAN AS SEEN BY THE SUPERCAM INSTRUMENT: EVIDENCE FOR A COMPLEX AQUEOUS HISTORY AND VARIABLE ALTERATION CONDITIONS.** E. Dehouck<sup>1\*</sup>, O. Forni<sup>2</sup>, C. Quantin-Nataf<sup>4</sup>, P. Beck<sup>3</sup>, N. Mangold<sup>4</sup>, O. Beyssac<sup>5</sup>, C. Royer<sup>6</sup>, E. Clavé<sup>7</sup>, J. R. Johnson<sup>8</sup>, L. Mandon<sup>3</sup>, F. Poulet<sup>10</sup>, A. Udry<sup>11</sup>, G. Lopez-Reyes<sup>12</sup>, G. Caravaca<sup>2</sup>, S. Maurice<sup>2</sup>, R. C. Wiens<sup>6</sup>, K. M. Stack<sup>13</sup>, R. B. Anderson<sup>14</sup>, S. Bernard<sup>5</sup>, T. Bosak<sup>15</sup>, A. P. Broz<sup>6</sup>, K. Castro<sup>16</sup>, S. M. Clegg<sup>17</sup>, A. Cousin<sup>2</sup>, G. Dromart<sup>1</sup>, K. A. Farley<sup>9</sup>, T. Fouchet<sup>18</sup>, J. Frydenvang<sup>19</sup>, T. S. J. Gabriel<sup>14</sup>, P. Gasda<sup>17</sup>, E. Gibbons<sup>20</sup>, B. H. N. Horgan<sup>6</sup>, J. A. Hurowitz<sup>21</sup>, H. Kalucha<sup>9</sup>, J. Lasue<sup>2</sup>, S. Le Mouélic<sup>4</sup>, J. M. Madariaga<sup>16</sup>, P.-Y. Meslin<sup>2</sup>, M. Nachon<sup>22</sup>, J. I. Nuñez<sup>8</sup>, P. Pilleri<sup>2</sup>, C. Pilorget<sup>10,23</sup>, J. W. Rice, Jr.<sup>24</sup>, P. S. Russell<sup>25</sup>, S. Schröder<sup>7</sup>, D. L. Shuster<sup>26</sup>, K. L. Siebach<sup>27</sup>, J. I. Simon<sup>28</sup>, B. P. Weiss<sup>15</sup>, A. J. Williams<sup>29</sup>, and the SuperCam team. <sup>1</sup>LGL-TPE, Lyon, France; <sup>2</sup>IRAP, Toulouse, Fr.; <sup>3</sup>IPAG, Grenoble, Fr.; <sup>4</sup>LPG, Nantes, Fr.; <sup>5</sup>IMPMC, Paris, Fr.; <sup>6</sup>Purdue Univ., West Lafayette, IN; <sup>7</sup>DLR, Berlin, Germany; <sup>8</sup>JHUAPL, Laurel, MD; <sup>9</sup>Caltech, Pasadena, CA; <sup>10</sup>IAS, Orsay, Fr.; <sup>11</sup>UNLV, Las Vegas; <sup>12</sup>Univ. Valladolid, Spain; <sup>13</sup>JPL, Pasadena, CA; <sup>14</sup>USGS, Flagstaff, AZ; <sup>15</sup>MIT, Cambridge, MA; <sup>16</sup>UPV/EHU, Leioa, Spain; <sup>17</sup>LANL, Los Alamos, NM; <sup>18</sup>LESIA, Meudon, Fr.; <sup>19</sup>Univ. Copenhagen, Denmark; <sup>20</sup>McGill Univ., Montréal, Canada; <sup>21</sup>Stony Brook Univ., NY; <sup>22</sup>Texas A&M Univ., College Station, TX; <sup>23</sup>IUF, Paris, Fr.; <sup>24</sup>ASU, Tempe, AZ; <sup>25</sup>UCLA, Los Angeles, CA; <sup>26</sup>UC Berkeley, CA; <sup>27</sup>Rice Univ., Houston, TX; <sup>28</sup>NASA JSC, Houston, TX; <sup>29</sup>Univ. Florida, Gainesville, FL. \*[erwin.dehouck@univ-lyon1.fr](mailto:erwin.dehouck@univ-lyon1.fr)

**Introduction:** In February 2021, the *Perseverance* rover landed in Jezero crater. The crater floor was found to be composed of lava flows and cumulate rocks that have undergone some limited aqueous alteration; however, it is not clear whether this alteration is related to the lacustrine phase of the crater [1-7]. After completing its exploration of these igneous units, *Perseverance* drove towards the sedimentary fan located at the mouth of Neretva Vallis, a river valley that incised the western rim of the crater [8]. Between April and December 2022, the rover investigated the basal layers of the fan in two areas named Cape Nukshak and Hawksbill Gap, which are ~400 m apart [9]. After building a contingency cache for Mars Sample Return in a flat area adjacent to the fan [10], *Perseverance* climbed onto and explored the upper surface of the fan from February to September 2023. Here, we present a synthetic view of the chemostratigraphy and mineralogy of the fan based on data collected throughout the traverse by the SuperCam instrument suite. We show that the fan records a strong compositional diversity, which in turn reflects a complex aqueous history and variable alteration conditions.

**Dataset:** SuperCam is a remote-sensing instrument that combines five different techniques to study various properties of the Martian rocks and soils [11,12]. Here, we use the major-element oxide compositions derived from the laser-induced breakdown spectroscopy (LIBS) data [13] to assess the chemical composition of the targets. We also use VISIR—i.e., visible (0.40–0.85  $\mu\text{m}$ ) and near-infrared (1.3–2.6  $\mu\text{m}$ )—reflectance spectra [6, 14], as well as some Raman measurements [15], to assess their mineralogical composition. The data shown here include only local rock targets, i.e., observations of float rocks, regolith, veins or coatings were set aside.

**Stratigraphic context:** All along the traverse, the Mars 2020 science team used rover imagery to examine the sedimentological properties of the rocks (grain size, color, geometry of laminae, erosion resistance, etc.) and define stratigraphic members and formations. The lowest

layers are part of the Shenandoah formation, described in [9]. Above are the Tenby and Otis Peak formations [16, 17]. Note that the Rockytop member, initially defined as the topmost member of the Shenandoah formation [9], is now included in the overlying Tenby formation [18].

**Results: Chemostratigraphy.** The LIBS-derived chemical compositions show that the western fan can be divided into three chemostratigraphic units (A, B and C; Fig. 1). Unit A corresponds to the lowest two members of the Shenandoah formation, named Kaguyak and Amalik (together ~1.1-m thick), which are only exposed in the Cape Nukshak section. These rocks are characterized by low  $\text{SiO}_2$  and  $\text{Al}_2\text{O}_3$  contents, high MgO content, and moderately high values of the (Fe+Mg)/Si molar ratio.

Unit B spans laterally between both the Cape Nukshak and Hawksbill Gap sections [9], and encompasses the remaining members of the Shenandoah formation. These rocks display higher  $\text{SiO}_2$  and  $\text{Al}_2\text{O}_3$  contents, lower MgO content, and lower (Fe+Mg)/Si ratio values compared to units A and C.

Finally, unit C encompasses the Tenby and Otis Peak formations, which appear chemically similar to each other despite their distinct sedimentological properties. These rocks are coarse-grained (granule sandstones to conglomerates) and thus show higher point-to-point variability in the LIBS measurements. Nonetheless, the average composition clearly shows a return to lower  $\text{SiO}_2$  and  $\text{Al}_2\text{O}_3$  contents, higher MgO content, and higher values of the (Fe+Mg)/Si molar ratio compared to unit B.

**Mineralogy.** Although the chemistry is relatively stable across several stratigraphic members, the VISIR measurements show that the mineralogy can be heterogeneous within a given chemostratigraphic unit.

Indeed, the two members composing unit A display VISIR signatures distinct from each other (Fig. 2). The mean spectrum of Kaguyak shows absorptions at 1.41, 1.93, 2.31, and 2.39  $\mu\text{m}$ , consistent with the presence of hydrated clay minerals and minor sulfates. In contrast, the spectrum of Amalik displays a reduced 1.93- $\mu\text{m}$  (hydra-

tion) band and a strong 2.33- $\mu\text{m}$  band; we attribute this signature to a Mg-rich serpentine (lizardite or antigorite).

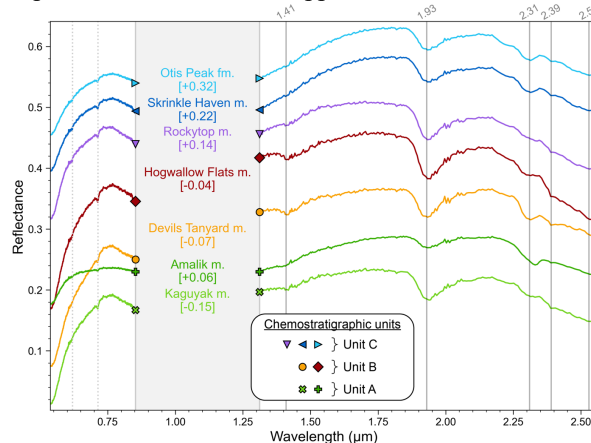
In unit B, the Devils Tanyard member displays a spectrum with absorption bands at 1.4, 1.9, 2.31 and 2.39  $\mu\text{m}$  indicative of Fe/Mg-bearing phyllosilicates. More specifically, the asymmetry of the 2.31- $\mu\text{m}$  band indicates the presence of Mg-rich vermiculite, likely mixed with some smectite. In contrast, the mean spectrum of the Hogwallow Flats member shows a shallower 2.3- $\mu\text{m}$  band, suggesting a reduced abundance of phyllosilicates, and a sharp drop of reflectance just shortward of 2.4  $\mu\text{m}$ . This feature, combined with enhanced sulfur detected by LIBS, indicates the presence of hydrated sulfates. An absorption at 433 nm further suggests the presence of Fe<sup>3+</sup>-bearing sulfates [19].

In unit C, the different members show more homogeneous VISIR spectra, mainly characterized by paired absorption bands at 2.3 and 2.5  $\mu\text{m}$  that are typical of carbonate minerals. The Rockytop member, however, displays a more unusual spectrum, with a strong 2.5- $\mu\text{m}$  band but a weak one at 2.3  $\mu\text{m}$ . Nonetheless, the Raman data confirm the presence of carbonates in Rockytop as well as in the overlying members [15]. In addition, the Raman data show the presence of olivine in most analyses performed within unit C.

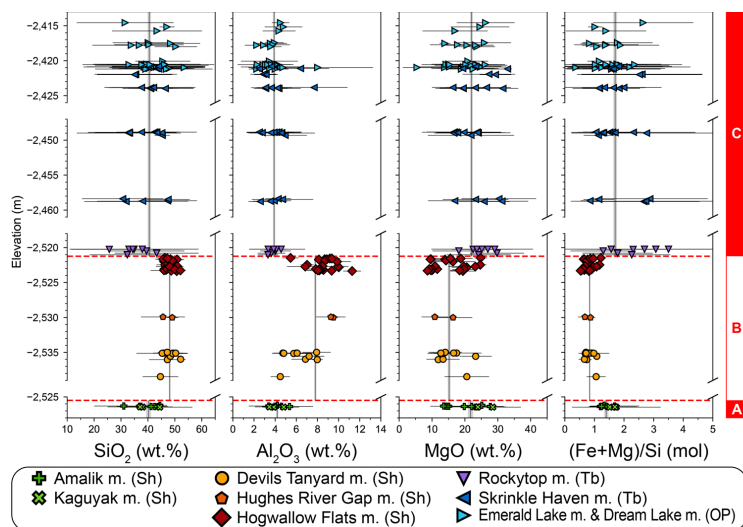
**Discussion:** Units A and C both show mafic to ultramafic compositions that are akin to the olivine-rich Séítah formation on the crater floor [3,5]. Although these two units show evidence for some secondary minerals in the VISIR data (mainly phyllosilicates and carbonates; Fig. 2), the chemical similarity with Séítah and the low Chemical Index of Alteration (CIA) values (average: 33.0 for unit A; 33.3 for unit C) suggest that only limited alteration occurred, or that it occurred at low water-to-rock ratio, strongly limiting the loss of mobile cations such as Fe<sup>2+</sup> and Mg<sup>2+</sup>. The persistence of abundant olivine in unit C is also an indication of limited alteration [e.g., 20].

In contrast, the chemical compositions measured in unit B deviate significantly from the rest of the fan stratigraphy. The enrichment in Al<sub>2</sub>O<sub>3</sub> (Fig. 1), and the resulting elevated CIA values (average: 49.5), indicate a change to either a weakly altered but highly evolved source material, or to more strongly altered sediments. Given that the CIA values would correspond to granite-like rocks, which are rare on Mars and not reported anywhere in the Jezero watershed, we favor the hypothesis that aqueous alteration is responsible for the distinctive chemical signature of the rocks forming unit B.

**Conclusion:** The boundary between units B and C corresponds to a transition from fine-grained bottomset/lacustrine deposits to coarser-grained foresets/topsets [21]. One possible model is that deposition of the latter occurred in a relatively short time and was quickly followed by a fall of the lake level and ultimately by the aridification of the crater, which put an end to the deposition of new sediments and to the aqueous alteration of the already-deposited sediments of the upper fan.



↑ **Figure 2** – Average VISIR spectra of the main stratigraphic units. Values in square brackets are the vertical offsets that have been applied to show the spectra in stratigraphic order.



← **Figure 1** – LIBS chemostratigraphic profile. Symbols correspond to average compositions per target (error bars = standard deviation). Vertical bars show the average compositions of the three chemostratigraphic units. (Sh = Shenandoah fm.; Tb = Tenby fm.; OP = Otis Peak fm.)

**References:** [1] Farley K. et al. (2022) *Science*. [2] Liu Y. et al. (2022) *Science*. [3] Wiens R. et al. (2022) *Sci. Adv.* [4] Udry A. et al. (2022) *JGR-P*. [5] Beyssac O. et al. (2022) *JGR-P*. [6] Mandon L. et al. (2022) *JGR-P*. [7] Clavé E. et al. (2022) *JGR-P*. [8] Fassett C. & Head J. (2005) *GRL*. [9] Stack K. M. et al. (2024) *JGR-P*. [10] MSR Campaign Science Group et al. (2023) *MAPS*. [11] Maurice S. et al. (2021) *Space Sci. Rev.* [12] Wiens R. et al. (2021) *Space Sci. Rev.* [13] Anderson R. et al. (2022) *Spectrochim. Acta B*. [14] Royer C. et al. (2022) *JGR-P*. [15] Clavé É. et al. (2024) *LPSC #1829*. [16] Siebach K. et al. (2024) *LPSC #2365*. [17] Gwizd S. et al. (2024) *LPSC #2117*. [18] Tice M. et al. (2024) *LPSC #2181*. [19] Johnson J. et al. (2023) *LPSC #1385*. [20] Olsen A. & Rimstidt J. (2007) *Am. Min.* [21] Mangold N. et al. (2024) *LPSC #1555*.